

Characterization of the continuous transition from atomic to molecular shape in the three-body Coulomb system

Laura D. Salas, Bárbara Zamora-Yusti, and Julio C. Arce*
Departamento de Química, Universidad del Valle, A.A. 25360, Cali, Colombia
 (Dated: September 13, 2021)

We present an alternative, univocal characterization of the continuous transition from atomic to molecular shape in the Coulomb system constituted by two identical particles and a third particle with the opposite charge, as the mass ratio of the particles varies. Applying a marginal-conditional exact factorization to a variationally optimized wavefunction, we construct a nonadiabatic potential energy surface for the relative motion between the single particle and each of the identical particles. The transition is revealed through the evolution with the mass ratio of the topography of such surface and of the shapes of the associated marginal and conditional distributions. Our approach unifies and extends to the nonadiabatic regime the Born-Oppenheimer and charge-distribution pictures of molecular shape.

I. INTRODUCTION

The paradigm of modeling molecules and solids as semi-rigid three-dimensional arrays of atoms held together by chemical bonds is inherited from the classical structural theory of chemistry [1, 2]. An obvious consequence of this picture is that molecules and repeat units in crystals are bestowed with the property of shape (see the entry ‘molecular shape’ in Ref. [3]). This property is fundamental for the interpretation of a wide variety of phenomena, like spectra of individual molecules [4], X-ray and neutron diffraction patterns from crystals [5], enzyme-substrate interactions [6], DNA replication and transcription [6], and solid-solid phase transitions [7], to name but a few.

On the other hand, in a fully ab initio quantum-mechanical theory those systems are treated as stable, isolated collections of electrons and (point) nuclei held together by electromagnetic forces [1, 2]. Specifically, the molecular Hamiltonian is entirely and uniquely determined just by the masses, charges and spins of all the constituent nuclei and electrons consistent with the molecular formula, without any a priori reference to atoms, bonds or shape [1, 2]. Consequently, geometrical symmetry does not feature among the symmetries exhibited by the molecular Hamiltonian [1, 2, 4]. Thus, *prima facie* the property of shape cannot be attributed to molecules and other compound quantal systems without recourse to auxiliary considerations [1, 2, 8–11].

In quantum chemistry, molecular shape is *imposed* by enforcing the clamped-nuclei constraint onto the Coulomb Hamiltonian, justified by the great difference between the masses of the nuclei and the electrons, from which a potential energy surface (PES) for the motion of the nuclei in the mean field of the electrons is constructed [12]. The topography of this hypersurface *defines* the shapes of all the structural isomers allowed by the molecular formula, by associating each one of them with an

isolated minimum (see the entry ‘equilibrium geometry’ in Ref. [3]). The region around a minimum, in turn, is employed to describe the quantized vibrations of the associated structural isomer [12]. Clearly, this melding of the ‘molecular structure hypothesis’ [1, 2] and quantum mechanics, called the Born-Oppenheimer (BO) approximation, does not *explain* molecular shape, since this property is not derived from first principles but is instead introduced in an ad hoc manner [12]. Therefore, although the validity of the BO approximation, with its associated construct of a PES, is not under question, there remains the challenge of clarifying to what extent and under what conditions the property of shape, in the sense employed in the molecular sciences, *emerges* in a quantal system from a fully ab initio treatment [1, 2, 8–11, 13–15].

Several viewpoints about this ‘molecular structure conundrum’ [16, 17] have been advanced, which we group, without any claim to completeness, into two categories: shape is either (1) an intrinsic property, i.e., it belongs to the isolated system, or (2) an extrinsic property, i.e., it is manifested through the interaction of the system with an external agent. In the intrinsic category there are three main classes: (1a) shape emerges from the correlations between all the constituent particles [10, 18–20]; (1b) molecular shape is a classical-like nuclear configuration arising from the decoherence induced on the nuclei by their interaction with the electrons [21, 22]; (1c) shape is a property entirely alien to stationary states, and can arise only in nonstationary states [1, 8]. In the extrinsic category there are also three main classes: (2a) the system acquires a well-defined shape only when it is considered together with its environment [1, 2, 8]; (2b) shape arises from the decoherence induced by the environment [23, 24]; (2c) shape is caused by the act of measurement performed by an observer on the system [25]. [Note that according to the decoherence theory of measurement [26] classes (2b) and (2c) would be equivalent.] Evidently, the problem of the emergence of shape is intimately related to the measurement problem and the classical limit of quantum mechanics [26]. Hence, a full resolution of the former is contingent upon the resolution of the latter, which is far from being accomplished [24]. The issue

* julio.arce@correounivalle.edu.co

is further complicated by the nuances in the concept of shape used by different authors.

In this paper we adhere to class (1a), that is, we seek to explain the emergence of molecular shape solely from the correlations between all the nuclei and electrons, treated on an equal footing, without invoking any internal decoherence mechanism. Moreover, we consider the system to be in a stationary state. Although a detailed discussion of the related notions of isolated molecule and stationary state is beyond the scope of this paper, we state our stance in this regard. First, by isolation we mean the limit of a hypothetical process where the dynamical interactions and the EPR correlations with the environment tend to zero, and we assume that this limit is well defined, as usual [2, 4]. Second, contrary to the view expressed in, e.g., Ref. [15], for an isolated quantum system time is an ill-defined concept, hence the basic dynamical law is the time-independent Schrödinger equation, not the time-dependent one. The latter can be shown to emerge when the system interacts with an environment in the classical limit (see, e.g., Ref. [27]). Therefore, an isolated quantum system must be in a stationary state. We focus on the simplest nontrivial system for which the property of molecular shape can be meaningfully ascribed, namely three particles interacting through Coulomb forces, two of them identical and the other one with the opposite charge, in the nonrelativistic ground state [19, 20, 28].

We had better begin by explaining what we mean by the shape of a quantal system. In Sec. II we make a critical assessment of the notion commonly adopted in the literature [18–20, 28] and then expound, in qualitative terms, our own view that we believe to be more general. Then, in Subsec. III A we apply our view to the three-particle system, exploiting the marginal-conditional exact factorization (MCEF) of the eigenfunction introduced earlier [29].

It may be considered a disadvantage of such ‘pre-BO’ [30] treatment that it has no place for a PES [12], such construct being so useful as an interpretive tool. In fact, in Ref. [29] we showed that an exact nonadiabatic PES (NAPES) [31–35] can be rigorously constructed *for the electrons* in the He atom, and that it has interpretive power, in particular for making connections with classical structure ideas. In Subsec. III B we apply this development to the three-particle system, which allows us to treat atoms and molecules on the same basis, complementing and enriching the discussion on the emergence of molecular shape.

In Sec. IV we implement our formalism for sequences of realistic (from H^- to H_2^+) and model three-particle systems. As in Refs. [19, 20, 36, 37] we examine the evolution of the system shape with the mass ratio of the single and double particles, which allows us to provide an alternative, univocal characterization of the transition from atomlike to moleculelike shape.

We close with Sec. V, where we provide concluding remarks and perspectives for future developments of this line of work.

II. THE NOTION OF SHAPE FOR A QUANTAL SYSTEM

Since the property of shape that we attribute to a classical (macroscopic) object is ultimately related to its particle distribution, it may seem fitting to consider the shape of a quantal system also as the shape of its particle distribution, in 3-dimensional physical space [18], which is experimentally observable [5]. Such quantity is encoded in the spatial probability density, obtained by marginalizing, i.e., integrating over, the spin variables in the squared modulus of the eigenfunction in the position representation. However, if the system has N particles and their coordinates are defined with respect to a stationary frame, the domain of this density will be a $3N$ -dimensional configuration space.

According to García-Sucre and Bunge [18], the particle distribution in physical space can be constructed from the one-particle marginal probability densities, defined by marginalizing the spatial probability density over the coordinates of all the particles but one,

$$\rho_i(\vec{q}) = \int' d^{3N-3} q' |\Phi(\vec{Q})|^2, \quad (1)$$

where \vec{Q} is a $3N$ -vector containing the coordinates of all the particles, \vec{q} is a 3-vector, and the prime indicates that the integral is to be performed over the configuration space that excludes the coordinates of the i -th particle. Naturally, if the system contains a subset of indistinguishable particles, their one-particle marginal densities will be identical. Maxima of one such density will indicate the most probable positions of the particle in physical space. Alternatively, instead of the one-particle marginal densities the extracule densities can be utilized, which have a similar interpretation but are defined in a different way, employing a reference point, commonly the center of mass [19, 20, 28, 38]. For a state with zero total angular momentum (S state) each maximum will actually constitute a 2-dimensional spherical shell centered at the center of mass [19, 28], due to the invariance of the Hamiltonian to overall spatial rotation [4]. These shells, considered independently, can provide partial information about the shape of the system. For example, for three-particle systems, Mátyus and coworkers have shown that a cut of the extracule density for the identical particles is sufficient to characterize the transition from atomic to molecular shape [19, 20]. (Incidentally, Ludeña and coworkers have demonstrated that the shape of the extracule density depends on the reference point selected for its definition, leaving a degree of ambiguity [36, 37].) The particle distribution is obtained by [18]

$$\rho(\vec{q}) = \sum_{i=1}^N \rho_i(\vec{q}), \quad (2)$$

which fulfills $\int d^3 q \rho(\vec{q}) = N$ if Φ is normalized to 1. According to the analysis of García-Sucre and Bunge,

the set of maxima of this density can be taken to define the shape of the system. In particular, for a semi-rigid molecule the set of regions of high nuclear density presumably correspond to the familiar ball-and-stick model. But this view overlooks the rotational invariance of the Hamiltonian and, with that, the fact that the shells associated with the maxima in the one-particle densities of several particles can strongly overlap (for an example see Ref. [20]). Even worse, these densities can have several maxima, causing all the possible nuclear configurations to be mixed up in the particle distribution, confusing the identification of the different structural isomers. Hence, such prescription does not work in general. The origin of this failure lies in the loss of information about the spatial relationships between a given particle and the rest of the particles implied by the marginalization entailed in the definition (1).

A generally unambiguous concept of shape is straightforward if we return to the original spatial probability density in $3N$ -dimensional configuration space. A point of this space corresponds to a possible configuration of the particles, i.e., a possible shape. Hence, a maximum of this function will correspond to a likely shape. In general, there will be more than one maximum, so the system will exhibit several possible shapes, but some shapes may be more probable than others. For simplicity, let us now focus on S states. The nuisance of the appearance of shells can be avoided by employing the interparticle distances as a set of internal coordinates [39], defining a relative configuration space of dimension $\dim = N(N-1)/2$, in terms of which the Hamiltonian is cast into a form manifestly invariant to overall translation, overall rotation, and coordinate inversion. The remaining symmetries of the full symmetry group of the Hamiltonian are the permutations of the space and spin coordinates within all sets of identical particles [4]. But still, even for a three-particle system ($\dim = 3$), the spatial probability density will be too complicated, making its analysis cumbersome. Therefore, it will be convenient to marginalize a chosen set of internal coordinates to obtain a reduced probability density in a relative configuration space of lower dimension, more amenable to visualization. If this set is chosen judiciously, the shape of the system can still be characterized univocally.

In the case of a molecule with N_n nuclei and possessing several semi-rigid structural isomers, marginalization of all the electron-electron and nucleus-electron distances from the full probability density will yield a purely nuclear probability density in a relative configuration subspace of $\dim = N_n(N_n-1)/2$. Each isolated maximum in this function will define a framework in one-to-one correspondence to the classical structure of a possible structural isomer. (If enantiomers are possible, there will be a maximum associated with each *pair* of them. Due to the invariance of the internal Hamiltonian to coordinate inversion, the eigenfunction can be chosen to have definite positive or negative parity. In that case, such maximum will correspond to the configuration of a superposition of

both enantiomers with positive or negative parity. This issue is related to the so-called Hund's paradox [1, 24].) The shape and breadth of one such maximum will contain the information about the natures and amplitudes of the distortions ('vibrations') of the entire corresponding nuclear framework. This notion of molecular shape conforms with what Claverie and Diner call 'quantum structure' [10], in contrast with the classical structure usually depicted as a ball-and-stick cartoon, sometimes with the balls replaced by thermal ellipsoids to represent the anisotropic vibrations [5]. It seems to us that this one-to-one correspondence between the quantum structure in $(N_n(N_n-1)/2)$ -dimensional nuclear relative configuration space and the classical structure in 3-dimensional physical space is all that is needed to account for the property of shape in an isolated molecule. Nevertheless, there still remains the 'conundrum' of why only one of the structural or optical isomers is observed in chemical experiments, which has elicited so much debate in the literature [1, 2, 8, 10, 11, 13–17, 24, 25]. (In this connection, it is well to keep in mind that in high-resolution spectroscopic experiments the molecule is nearly isolated, so that it can be considered to be in an eigenstate, whereas in chemical experiments it is interacting with an environment, so that it must be considered to be in a statistical mixture [1, 23, 24].)

III. THE MARGINAL-CONDITIONAL EXACT FACTORIZATION FORMALISM

A. The shape of the three-particle system

Let us now specialize these ideas to our three-particle system. We consider the charges $q_1 = q_2 = -q_3$ (according to charge conjugation invariance, it is immaterial whether q_3 is positive or negative). Thus, the masses $m_1 = m_2 < m_3$ model an atomlike system, with the identical particles playing the role of the electrons, whereas the masses $m_1 = m_2 > m_3$ model a moleculelike system, with the identical particles playing the role of the nuclei. The only symmetry of the Hamiltonian that needs explicit consideration is the permutation of the spatial and spin coordinates of particles 1 and 2. We assume that these particles are fermions, so that the eigenfunction must be antisymmetric under this operation.

For an S state the internal coordinates are r_{12}, r_{13}, r_{23} , where r_{ij} is the distance between particles i and j [39–42]. They determine the shape and size of the triangle defined by the positions of the three particles, and are independent, except that they are constrained by the triangle condition $|r_{13} - r_{23}| \leq r_{12} \leq r_{13} + r_{23}$. The volume element of this configuration space is $dV = r_{12}r_{13}r_{23}dr_{12}dr_{13}dr_{23}$.

The eigenfunction can be written as the product of a spatial part, $\Phi(r_{12}, r_{13}, r_{23})$, and a spin eigenfunction which, in turn, is the product of a spin function for particles 1 and 2 and a spin function for particle 3 [43].

Evidently, in this case the marginalization of the spin variables in the probability density amounts to working only with the spatial eigenfunction, since the spin eigenfunction is normalized. Hence, the shape of this system is encoded in the joint distribution function

$$D(r_{12}, r_{13}, r_{23}) = r_{12}r_{13}r_{23}|\Phi(r_{12}, r_{13}, r_{23})|^2 \quad (3)$$

(which includes the Jacobian because it is a radial probability density). We marginalize the distance between the identical particles, r_{12} , to obtain a 2-dimensional marginal distribution (MD) for finding particles 1 and 2 at distances r_{13} and r_{23} from particle 3, respectively, *regardless* of r_{12} (here and henceforth, when we speak of the probability of finding two particles at a certain distance, we imply within an infinitesimal neighborhood around that distance),

$$D_m(r_{13}, r_{23}) := \int_{|r_{13}-r_{23}|}^{r_{13}+r_{23}} dr_{12}r_{12}D(r_{12}, r_{13}, r_{23}). \quad (4)$$

Note that if we marginalized two of the distances we would obtain a 1-dimensional MD that obviously could not provide, by itself, information about the shape of the system. Now, according to Bayes' product rule, the joint distribution can be factorized exactly as

$$D(r_{12}, r_{13}, r_{23}) = D_m(r_{13}, r_{23})D_c(r_{12}|r_{13}, r_{23}), \quad (5)$$

where D_c is the conditional distribution (CD) function for finding particles 1 and 2 at a distance r_{12} , *provided* they are found at distances r_{13} and r_{23} from particle 3, respectively. Taking into account the normalization of D ,

$$\int_0^\infty dr_{13}r_{13} \int_0^\infty dr_{23}r_{23} \times \int_{|r_{13}-r_{23}|}^{r_{13}+r_{23}} dr_{12}r_{12}D(r_{12}, r_{13}, r_{23}) = 1, \quad (6)$$

and imposing that D_m be normalized in the $\{r_{13}, r_{23}\}$ configuration subspace,

$$\int_0^\infty dr_{13}r_{13} \int_0^\infty dr_{23}r_{23}D_m(r_{13}, r_{23}) = 1, \quad (7)$$

imply that D_c is *locally* normalized at every point of this subspace,

$$\int_{|r_{13}-r_{23}|}^{r_{13}+r_{23}} dr_{12}r_{12}D_c(r_{12}|r_{13}, r_{23}) = 1. \quad (8)$$

When evaluated at selected points (r_{13}, r_{23}) the CD becomes a 1-dimensional function that can also aid in the analysis. (It is worth mentioning that Berry and coworkers have employed 2-dimensional CD's defined in an ad hoc way, by fixing the distance between one electron and the nucleus in the joint distribution, to illustrate that two-valence-electron atoms acquire a moleculelike shape in some states [44].)

B. The nonadiabatic potential energy surface

The structure of our nonrelativistic three-particle system in an S state is governed by the internal Schrödinger equation [39–42]

$$\hat{H}\Phi(r_{12}, r_{13}, r_{23}) = E\Phi(r_{12}, r_{13}, r_{23}). \quad (9)$$

In atomic units ($\hbar = m_e = e = 1$), the spin-free Hamiltonian reads [39, 42]

$$\begin{aligned} \hat{H} = & -\frac{1}{2\mu_{12}} \left(\frac{\partial^2}{\partial r_{12}^2} + \frac{2}{r_{12}} \frac{\partial}{\partial r_{12}} \right) - \frac{1}{2\mu_{13}} \left(\frac{\partial^2}{\partial r_{13}^2} + \frac{2}{r_{13}} \frac{\partial}{\partial r_{13}} \right) - \frac{1}{2\mu_{23}} \left(\frac{\partial^2}{\partial r_{23}^2} + \frac{2}{r_{23}} \frac{\partial}{\partial r_{23}} \right) \\ & + \frac{q_1 q_2}{r_{12}} + \frac{q_1 q_3}{r_{13}} + \frac{q_2 q_3}{r_{23}} \\ & - \frac{1}{m_1} \frac{r_{12}^2 + r_{13}^2 - r_{23}^2}{2r_{12}r_{13}} \frac{\partial^2}{\partial r_{12}\partial r_{13}} - \frac{1}{m_2} \frac{r_{23}^2 + r_{12}^2 - r_{13}^2}{2r_{23}r_{12}} \frac{\partial^2}{\partial r_{23}\partial r_{12}} - \frac{1}{m_3} \frac{r_{13}^2 + r_{23}^2 - r_{12}^2}{2r_{13}r_{23}} \frac{\partial^2}{\partial r_{13}\partial r_{23}}, \end{aligned} \quad (10)$$

where m_i and q_i are the mass and charge of particle i ,

$$\frac{1}{\mu_{ij}} \equiv \frac{1}{m_i} + \frac{1}{m_j} \quad (11)$$

defines the reduced mass of particles i and j , and naturally $r_{ij} = r_{ji}$. Note that the first and second lines contain the contributions of each particle pair to the kinetic energy and the Coulombic potential energy, respec-

tively, while the third line contains the kinetic couplings between the particle pairs.

We aim at constructing a NAPES for the degrees of freedom included in the MD, namely, r_{13} and r_{23} . The procedure is analogous to the one presented in ref. [29], making the correspondences $r_1 \rightarrow r_{13}$, $r_2 \rightarrow r_{23}$, $r_{12} \rightarrow r_{12}$, and using the Hamiltonian (10) instead of the fixed-nucleus Hamiltonian. Hence, here we present only the

most relevant equations and interpretations, and refer the reader to Ref. [29] for further details. Following Hunter [31], we introduce the MCEF of the spatial eigenfunction [29]

$$\Phi(r_{12}, r_{13}, r_{23}) = \psi(r_{13}, r_{23})\chi(r_{12}|r_{13}, r_{23}), \quad (12)$$

by defining marginal and conditional amplitudes

$$\begin{aligned} \psi(r_{13}, r_{23}) &:= e^{i\theta(r_{13}, r_{23})} \\ &\times \left[\int_{|r_{13}-r_{23}|}^{r_{13}+r_{23}} dr_{12} r_{12} |\Phi(r_{12}, r_{13}, r_{23})|^2 \right]^{1/2} \\ &\equiv e^{i\theta(r_{13}, r_{23})} \langle \Phi | \Phi \rangle^{1/2}, \end{aligned} \quad (13)$$

$$\chi(r_{12}|r_{13}, r_{23}) := \frac{\Phi(r_{12}, r_{13}, r_{23})}{\psi(r_{13}, r_{23})}, \quad (14)$$

where, from here onwards, angular brackets express integrals over r_{12} with the Jacobian r_{12} . The phase $\exp[i\theta(r_{13}, r_{23})]$, with θ real, is arbitrary and can be chosen to set the symmetries of ψ and χ with respect to the exchange $r_{13} \leftrightarrow r_{23}$ [29, 34]. Now we can write

$$D_m(r_{13}, r_{23}) = r_{13}r_{23}|\psi(r_{13}, r_{23})|^2, \quad (15)$$

$$D_c(r_{12}|r_{13}, r_{23}) = r_{12}|\chi(r_{12}|r_{13}, r_{23})|^2, \quad (16)$$

which, together with Eqs. (6)-(8), imply the normaliza-

tion conditions

$$\int_0^\infty dr_{13} r_{13} \int_0^\infty dr_{23} r_{23} \langle \Phi | \Phi \rangle = 1, \quad (17)$$

$$\int_0^\infty dr_{13} r_{13} \int_0^\infty dr_{23} r_{23} |\psi|^2 = 1, \quad (18)$$

$$\langle \chi | \chi \rangle = 1. \quad (19)$$

The local normalization of χ , Eq. (19), guarantees that the MCEF (12) is unique, within the arbitrary phase mentioned above [34].

To derive the equations that govern ψ and χ we apply the variational principle, as follows. First, we set up the constrained functional [29, 34]

$$\begin{aligned} F[\Phi] &\equiv \int_0^\infty dr_{13} r_{13} \int_0^\infty dr_{23} r_{23} \langle \Phi | \hat{H} | \Phi \rangle \\ &- \int_0^\infty dr_{13} r_{13} \int_0^\infty dr_{23} r_{23} \lambda(r_{13}, r_{23}) (\langle \chi | \chi \rangle - 1) \\ &- \epsilon \left(\int_0^\infty dr_{13} r_{13} \int_0^\infty dr_{23} r_{23} |\psi|^2 - 1 \right), \end{aligned} \quad (20)$$

where the first term is the expectation value of the energy, the second term enforces the local normalization of χ , and the third term enforces the normalization of ψ , with $\lambda(r_{13}, r_{23})$ and ϵ being Lagrange multipliers. Then we impose the extremization condition $\delta F = 0$, which yields [29]

$$[\hat{T}_{13,23} + U(r_{13}, r_{23})] \psi(r_{13}, r_{23}) = E \psi(r_{13}, r_{23}), \quad (21)$$

$$\hat{\Omega}[\psi] \chi(r_{12}|r_{13}, r_{23}) = U(r_{13}, r_{23}) \chi(r_{12}|r_{13}, r_{23}), \quad (22)$$

where

$$\hat{T}_{13,23} \equiv -\frac{1}{2\mu_{13}} \left(\frac{\partial^2}{\partial r_{13}^2} + \frac{2}{r_{13}} \frac{\partial}{\partial r_{13}} \right) - \frac{1}{2\mu_{23}} \left(\frac{\partial^2}{\partial r_{23}^2} + \frac{2}{r_{23}} \frac{\partial}{\partial r_{23}} \right), \quad (23)$$

$$\begin{aligned} \hat{\Omega}[\psi] &\equiv \hat{H} - \frac{1}{\mu_{13}} \frac{1}{\psi} \frac{\partial \psi}{\partial r_{13}} \frac{\partial}{\partial r_{13}} - \frac{1}{\mu_{23}} \frac{1}{\psi} \frac{\partial \psi}{\partial r_{23}} \frac{\partial}{\partial r_{23}} \\ &- \frac{1}{m_1} \frac{r_{12}^2 + r_{13}^2 - r_{23}^2}{2r_{12}r_{13}} \left(\frac{1}{\psi} \frac{\partial \psi}{\partial r_{13}} \frac{\partial}{\partial r_{12}} \right) - \frac{1}{m_2} \frac{r_{12}^2 + r_{23}^2 - r_{13}^2}{2r_{12}r_{23}} \left(\frac{1}{\psi} \frac{\partial \psi}{\partial r_{23}} \frac{\partial}{\partial r_{12}} \right) \\ &- \frac{1}{m_3} \frac{r_{13}^2 + r_{23}^2 - r_{12}^2}{2r_{13}r_{23}} \left(\frac{1}{\psi} \frac{\partial \psi}{\partial r_{23}} \frac{\partial}{\partial r_{13}} + \frac{1}{\psi} \frac{\partial \psi}{\partial r_{13}} \frac{\partial}{\partial r_{23}} + \frac{\partial^2 \psi}{\partial r_{13} \partial r_{23}} \right), \end{aligned} \quad (24)$$

and the notation $\hat{\Omega}[\psi]$ indicates that this operator depends on $\psi(r_{13}, r_{23})$. The eigenvalues E and $U(r_{13}, r_{23})$ are related to the Lagrange multipliers and to each other

by [29]

$$E = \epsilon = \int_0^\infty dr_1 r_1 \int_0^\infty dr_2 r_2 \lambda(r_{13}, r_{23}), \quad (25)$$

$$U(r_{13}, r_{23}) \equiv \frac{\lambda(r_{13}, r_{23})}{|\psi(r_{13}, r_{23})|^2} - \frac{\hat{T}_{13,23} \psi(r_1, r_2)}{\psi(r_{13}, r_{23})}. \quad (26)$$

We have conveniently arranged Eqs. (21) and (22) so as to expose their analogy with the BO vibrational and

clamped-nuclei electronic equations, respectively: r_{12} and $\{r_{13}, r_{23}\}$ are analogous to the electronic and the nuclear coordinates, respectively; $\hat{\Omega}[\psi]$ and $\hat{T}_{13,23}$ are analogous to the clamped-nuclei Hamiltonian and the nuclear kinetic energy operator, respectively; χ and ψ are analogous to the electronic and the vibrational eigenfunctions, respectively; and $U(r_{13}, r_{23})$ is analogous to the BO PES, which is the sought-after NAPES. It must be kept in mind that, due to the uniqueness of the MCEF, there can be only one marginal (‘vibrational’) eigenfunction, with total energy E , associated with this NAPES, in contrast with the BO case, where the same PES can support a number of vibrational states with different total energies. In addition, for an atomlike system Eq. (21) has the form of an *exact* central-field model, with $U(r_{13}, r_{23})$ being the effective radial potential [29]. It is very significant that our two main interpretive tools, the MD and the NAPES, turn out to be rigorously related by Eq. (21) together with Eq. (15). In fact, we can regard Eq. (21) as a Schrödinger equation with potential $U(r_{13}, r_{23})$ and eigenfunction $\sqrt{D_m(r_{13}, r_{23})}/r_{13}, r_{23}$.

IV. CALCULATIONS AND DISCUSSION

We studied the atomlike-moleculelike transition of the ground state along a sequence of systems composed of three singly-charged particles. Such state ought to be a singlet ($S = 0$) with respect to the total spin of the two identical particles, which implies that the spatial eigenfunction (12) must be symmetric with respect to the exchange $r_{13} \leftrightarrow r_{23}$. We set $\theta \equiv 0$, so that both ψ and χ are also symmetric [see Eqs. (13) and (14)].

We considered the sequence of realistic, albeit most of them exotic, systems H^- ($e^-e^-p^+$), Mu^- ($e^-e^-\mu^+$), Ps^- ($e^-e^-e^+$), Mu_2^+ ($\mu^+\mu^+e^-$), H_2^+ ($p^+p^+e^-$). [Note that Ps^- and Ps_2^+ ($e^+e^+e^-$) are equivalent for our purposes.] He ($e^-e^-\alpha^{2+}$) is not included in this sequence, since the alpha particle is doubly charged. We discussed its NAPES and distribution functions in detail in Ref. [29]. Here, we make reference to this system when it helps illuminate the discussion. Since in the sequence (e^\pm, μ^\pm, p^\pm) the mass changes too abruptly, in order to visualize the transition in a smoother way we also considered a series of model systems within a relatively narrow range of the parameter $R \equiv m_s/m_d$, where m_s and m_d are the masses of the single and double particles, respectively.

From the practical standpoint, solving the nonlinear system of Eqs. (21) and (22) does not seem any easier than solving the original Schrödinger equation (9) [45, 46]. Hence, our strategy consists of extracting approximate marginal and conditional amplitudes from a variationally optimized wavefunction, using Eqs. (13) and (14), and then evaluating the NAPES by

$$U(r_{13}, r_{23}) = \langle \chi | \hat{\Omega}[\psi] | \chi \rangle, \quad (27)$$

in accordance to Eq. (22).

We employed the trial function of Flores-Riveros and Rivas-Silva [47]

$$\Phi(r_{13}, r_{23}, r_{12}) = (e^{-\alpha r_{13} - \beta r_{23}} + e^{-\beta r_{13} - \alpha r_{23}}) \times e^{-\gamma(r_{12} - u_0)^2} r_{12}^l, \quad (28)$$

where $\alpha, \beta, \gamma, u_0 \in \mathbb{R}^+$ and $l \in \mathbb{Z}^{0+}$ are variational parameters. We selected this simplistic trial function because it is amenable to a clear physical interpretation. Namely, for atomlike systems the first factor has the form of the Hylleraas unrestricted (different orbitals for different electrons) ansatz for the two-electron atom [40]. On the other hand, to interpret this factor for moleculelike systems let us take α as the larger of the two exponential parameters. Then, when α is sufficiently larger than β , so that the exponentials that contain β remain close to 1 in the range where the accompanying exponentials containing α decay to nearly zero, the function resembles the simple linear combination of atomic orbitals – molecular orbital (LCAO-MO) approximation, $1s_1(r_{13}) + 1s_2(r_{23})$, of the $1\sigma_g$ MO [43]. The second factor is a ground-state harmonic-oscillator-type eigenfunction that describes vibrational motion along r_{12} about the equilibrium distance u_0 . For atomlike systems it plays the role of a Gaussian geminal correlation factor, while for moleculelike systems it represents the harmonic vibration of the nuclei. The third factor introduces anharmonicity into that motion when $l > 0$. Moreover, the evolution of the variational parameters with R aids in the characterization of the transition, as follows. The overall extension of the system is controlled by β : the smaller the value of β the larger the extension. On the other hand, the relative localization of the two identical particles within a given system is controlled by γ : the larger γ the higher the localization. We can claim that the degree of this localization, in comparison with the overall extension, is indicative of the atomlike or moleculelike character of the system, since we know that the interelectronic motion in the atom is relatively loose, whereas the internuclear motion in the molecule is relatively tight. Therefore, we can employ the ratio β/γ as a diagnostic of the progress of the transition along the sequence of systems. In particular, we expect that this ratio decrease as the system becomes more moleculelike.

A further advantage of the trial function (28) is that all of our calculations can be done analytically, which we achieved with the aid of Wolfram Mathematica 12.0 [48]. Nevertheless, the expressions are extremely formidable, so we will not show them here.

Table I displays the optimal values of the variational parameters for the sequence of realistic systems (He is included for comparison purposes). It is seen that for the atomic systems Mu^- and H^- ($R \gg 1$) $\alpha \simeq 2\beta$, with $\alpha > 1$. A common interpretation of this relationship is that the atom has an inner electron suffering a negative screening, which makes it more strongly bound than the outer electron suffering a positive screening [38, 40]. On the other hand, for the molecular systems Mu_2^+ and H_2^+

TABLE I. Optimized variational parameters in the trial function (28) for the realistic systems. α, β, γ and u_0 are given in atomic units.

	$R = m_s/m_d$	α	β	γ	β/γ	u_0	l
He	7294	2.20740	1.41173	0.03253	43.4	4.45774	0
H ⁻	1836	1.07324	0.47322	0.00957	49.4	11.49397	0
Mu ⁻	206.8	1.06758	0.46882	0.00957	49.0	11.41274	0
Ps ⁻	1.000	0.52109	0.15209	0.00744	20.4	8.18378	0
Mu ₂ ⁺	0.004836	1.11320	0.21525	1.32386	0.16	1.76860	2
H ₂ ⁺	0.000540	1.12988	0.21672	4.87807	0.044	1.93988	2

TABLE II. Realistic systems. E_{exact} is the ‘exact’ energy (the sources of these values can be found in ref. [47]), $\langle E \rangle$ is the energy expectation value, U_e, U^\ddagger and $(r_{13,e}, r_{23,e})$ are the energy of the minima, the energy of the saddle point, and the coordinates of a minimum (the coordinates of the other minimum are obtained by interchanging these values) in the NAPES, respectively, and $(r_{13,m}, r_{23,m})$ are the coordinates of the maximum ($r_{13,m} = r_{23,m}$) or one of the maxima ($r_{13,m} \neq r_{23,m}$; the coordinates of the other maximum are obtained by interchanging these values) in the MD. All values are given in atomic units.

	E_{exact}	$\langle E \rangle$	U_e	U^\ddagger	$r_{13,e}, r_{23,e}$	$r_{13,m}, r_{23,m}$
He	-2.903	-2.902	-7.601	-7.286	0.26 0.43	0.61 0.61
H ⁻	-0.527	-0.525	-1.594	-0.992	0.48 12.09	1.54 1.54
Mu ⁻	-0.525	-0.523	-1.586	-0.986	0.49 12.03	1.55 1.55
Ps ⁻	-0.262	-0.260	-0.792	-0.416	0.99 11.72	3.26 3.31
Mu ₂ ⁺	-0.585	-0.583	-3.829	-2.065	0.35 2.20	0.76 1.99
H ₂ ⁺	-0.597	-0.596	-7.544	-4.484	0.25 2.05	0.75 1.71

($R \ll 1$) $\alpha \simeq 5\beta$, in accordance to the LCAO-MO interpretation given above. (For H₂⁺, it is interesting to note that our results for α, β , and u_0 are close to the ones of the simple LCAO-MO treatment, $\alpha = 1.24$ and $\beta \equiv 0$ at $R_e = 2.00$ bohr. [43].) Finally, for Ps⁻ ($R = 1$) $\alpha \simeq 3.4\beta$, so this system can be expected to be somewhat intermediate between atomic and molecular. In addition, for systems with $R > 1$ or $R < 1$, it is obtained that $l = 0$ or $l = 2$, respectively, which means that in the atomic systems the interelectronic motion is harmonic, whereas in the molecular systems the internuclear motion is anharmonic. Furthermore, it is seen that along the sequence β/γ decreases (recall that He does not belong in this sequence), as predicted above, and that for the atomic systems $\beta/\gamma \gg 1$, whereas for the molecular systems $\beta/\gamma \ll 1$.

Table II presents the expectation value of the energy obtained from the trial function (28) and the ‘exact’ non-relativistic energy for the realistic systems. The level of agreement is sufficient for our largely qualitative analysis. Employing more accurate trial functions (see, e.g., Ref. [28]) does not produce any relevant qualitative changes in the features of the NAPES’s and MD’s to be discussed below, as demonstrated in ref. [29] (a similar observation was made for the computed one-particle densities in Ref. [20]), but might instead obscure the interpretation.

Table III shows the optimal values of the variational parameters for the sequence of model systems, characterized by $R = m_s$ since the mass of the double particle was kept at $m_d = 1$ atomic unit. It is observed that as R goes

TABLE III. Optimized variational parameters in the trial function (28) for the model systems. α, β, γ and u_0 are given in atomic units. $l = 0$ in all cases.

$R = m_s$	α	β	γ	u_0
2.000	0.69797	0.23174	0.00850	8.20320
1.750	0.66546	0.21561	0.00836	8.05929
1.500	0.62658	0.19699	0.00810	8.02482
1.250	0.57969	0.17637	0.00801	7.95740
1.000	0.52109	0.15209	0.00744	8.18378
0.750	0.44661	0.12358	0.00685	8.59581
0.500	0.34870	0.08771	0.00608	9.49008
0.375	0.28541	0.07078	0.00501	11.38755
0.250	0.21056	0.04927	0.00390	14.45530
0.150	0.13915	0.03016	0.00266	19.74359

from 2.000 to 0.150 (a much smaller range than the one considered in Table I), the ratio α/β goes smoothly from 3.0 to 4.6, the same increasing trend seen in Table I, associated with the transition from atomlike to moleculelike structure. In addition, for the atomlike systems ($R > 1$) the equilibrium ‘interelectronic’ distance (u_0) increases slightly with the mass of the ‘nucleus’ (m_s). This is due to the fact that as the nucleus becomes less mobile it is a little less effective at screening the electrons from one another. On the other hand, for the moleculelike systems ($R < 1$) the equilibrium ‘internuclear’ distance (u_0) decreases rather strongly with the mass of the ‘electron’ (m_s). This is due to the fact that as the electron

becomes less mobile, it is more effective at binding the nuclei. Moreover, it is observed that across the transition β/γ decreases monotonically (from 27.3 to 11.3), as expected from the previous discussion.

Table IV displays the expectation value of the energy for the model systems. It is observed that as the mass of the single particle decreases $\langle E \rangle$ increases monotonically, i.e., the system becomes less stable. This can be attributed to the increase in the contribution of the single particle to the kinetic energy [see Eq. (10)].

TABLE IV. Model systems. $\langle E \rangle$ is the energy expectation value, $(r_{13,m}, r_{23,m})$ are the coordinates of the maximum ($r_{13,m} = r_{23,m}$) or one of the maxima ($r_{13,m} \neq r_{23,m}$; the coordinates of the other maximum are obtained by interchanging these values) in the MD, and SD is the second derivative at the maximum or at the middle point between the two maxima of the MD cuts of Fig. 4. All values are given in atomic units.

$R = m_s$	$\langle E \rangle$	$r_{13,m}, r_{23,m}$		SD
2.000	-0.346	2.43	2.43	-0.002059
1.750	-0.330	2.55	2.55	-0.001446
1.500	-0.311	2.72	2.72	-0.000821
1.250	-0.288	2.94	2.94	-0.000320
1.000	-0.260	3.26	3.31	0.000022
0.750	-0.223	3.39	4.40	0.000250
0.500	-0.174	3.84	6.47	0.000274
0.375	-0.144	4.46	8.43	0.000170
0.250	-0.106	5.73	11.92	0.000071
0.150	-0.070	8.39	17.44	0.000018

Figure 1 shows the NAPES's for the sequence of realistic systems and Table II contains data about the relevant topographical features of these surfaces. It is appreciated that for H^- , Mu^- and Ps^- they resemble the one for He discussed in Ref. [29]. In particular, they exhibit two perpendicular basins, separated by a ridge along the $r_{13} = r_{23}$ diagonal which goes asymptotically to zero. A classical interpretation of the topography of such a surface implies that the minima correspond to two broken-symmetry indistinguishable equilibrium structures (so-called versions [4]) with an inner electron and an outer electron [38, 40]. The saddle point that separates the two basins along the minimum potential energy path corresponds to a symmetric structure with the two electrons on the same orbit. On the other hand, the NAPES's for Mu_2^+ and H_2^+ exhibit two nearly parallel basins originating at relatively narrow wells and separated by a plateau centered at the $r_{13} = r_{23}$ diagonal and that approaches zero asymptotically. Interestingly, when the internuclear repulsion is removed from $\hat{\Omega}$ [see Eqs. (24) and (27)], these NAPES's change very little, in contrast with the atomic case, where removal of the interelectronic repulsion from $\hat{\Omega}$ causes the ridge to disappear [29]. In a classical interpretation of this topography, the minima correspond to two versions of a broken-symmetry equilibrium structure, where one of the nuclei orbits the electron more

closely than the other. These two minima are separated by a saddle point that corresponds to a symmetric structure with the two nuclei remaining at the same distance from the electron. Evidently, for a moleculelike system this NAPES provides explicit information about the relative motion between each nucleus and the electron, with the internuclear motion averaged out, in contrast with the customary BO potential energy *curve*, which provides explicit information about the internuclear motion in the mean field of the electron [43].

To envision classical motion over such a NAPES, only trajectories with total energy $\langle E \rangle$ ($\simeq E$) are allowed. In addition, since the wavefunction (28) is symmetric with respect to the exchange $r_{13} \leftrightarrow r_{23}$, such motion must be constituted by in-phase breathings of the orbits at all times. For example, in the atomic case a straight trajectory running along a basin is permitted, as it corresponds to one orbit breathing along r_{i3} with the other one frozen at $r_{j3} = \text{constant}$. In the molecular case, on the other hand, a straight trajectory running along a basin involves an in-phase breathing of both orbits, since the basins run nearly along diagonals, which corresponds to a symmetric vibrational mode. In both cases, as the total energy lies above the saddle point (see Table II), the two versions can actually interconvert via trajectories that cross the $r_{13} = r_{23}$ diagonal (a so-called degenerate rearrangement [4]). In the atomic case the asymptotic limit along a basin ($r_{j3} = \text{constant}$, $r_{i3} \rightarrow \infty$) would correspond to ionization with the other electron's orbit frozen, while in the molecular case the asymptotic limit along a basin ($r_{13}, r_{23} \rightarrow \infty$) would correspond to complete break up of the system, but these limits are in fact unreachable since the state is bound.

Figure 1 also displays the corresponding MD's for the realistic systems and Fig. 2 shows the MD for the He atom, for comparison purposes. It is helpful to imagine D_m 'sitting' on U . It is seen that for He, H^- , and Mu^- such distribution is unimodal, with its maximum located on the diagonal, i.e. with both electrons on the same orbit, whereas for Mu_2^+ and H_2^+ such distribution is bimodal, with each hump located more or less on top of a well (see Table II). Hence, the symmetry breaking implied by the NAPES topography is frustrated in the shape of the atomlike systems, that is, there is no inner-outer separation of the electrons, while it is manifested in the shape of the moleculelike systems. (Interestingly, a similar symmetry breaking arises in a fictitious model of He as the *interelectronic repulsion* is enhanced [29].) Evidently, this symmetry breaking in the moleculelike systems is far from sharp, in the sense that configurations where one of the nuclei orbits the electron closer than the other are only slightly preferred over configurations where both nuclei are on the same orbit. In other words, the probability of finding the electron at the same distance from the two nuclei is less than the probability of finding it closer to one of the nuclei. This is in accordance with the well-known characteristics of the covalent bond in H_2^+ [43]. In the case of Ps^- , the MD turns out to be

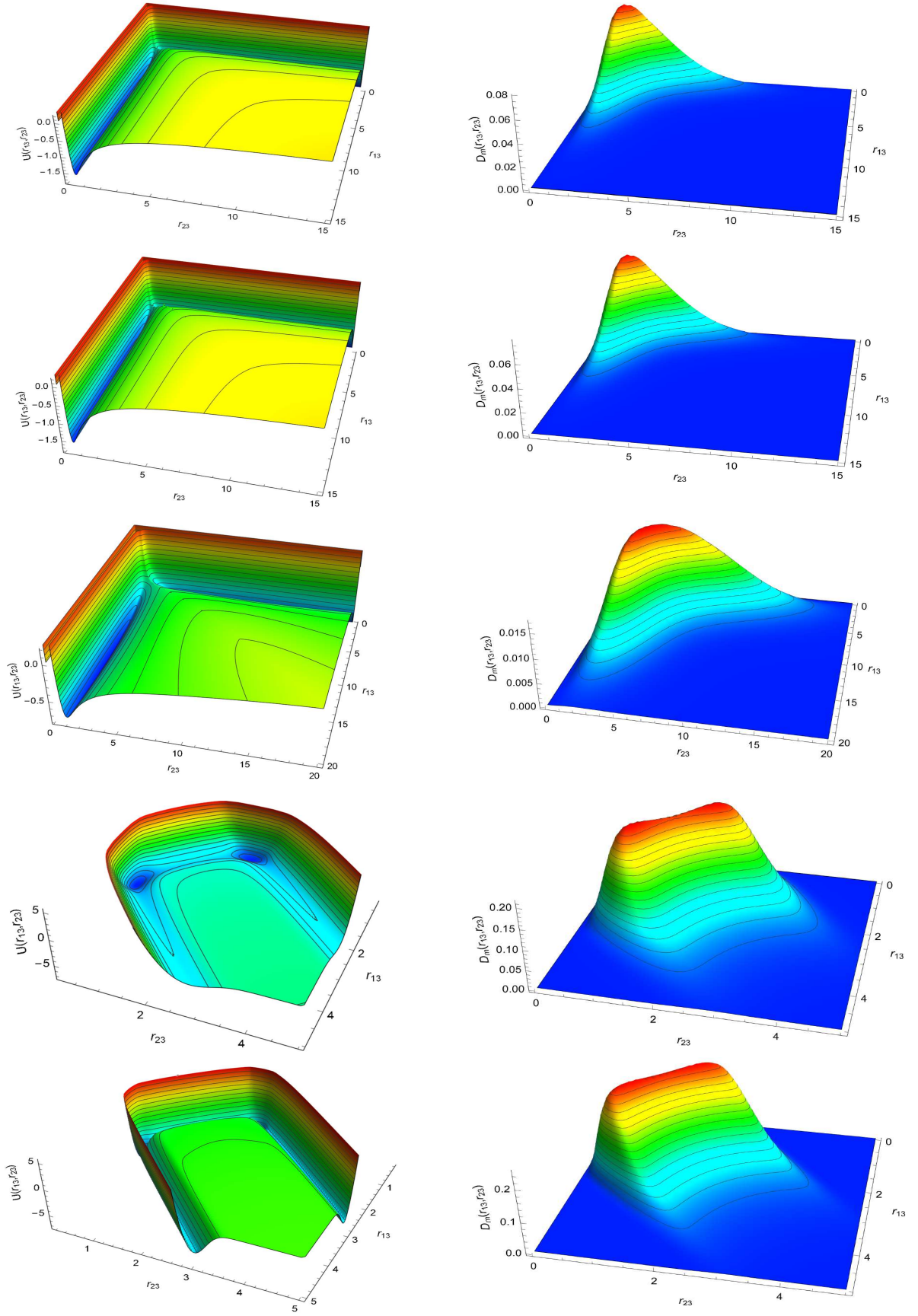


FIG. 1. (Color online) NAPES's (left column) and corresponding MD's (right column) for the realistic systems. From top to bottom: H^- , Mu^- , Ps^- , Mu_2^+ , H_2^+ .

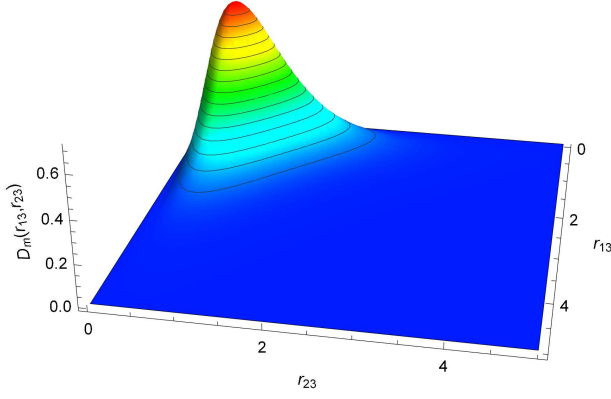


FIG. 2. (Color online) MD for the He atom.

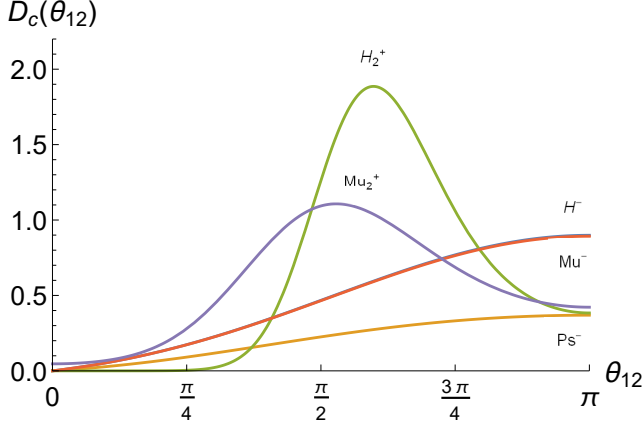


FIG. 3. (Color online) CD's for the realistic systems evaluated at the maximum or one of the maxima of the corresponding MD for the atomlike or moleculelike cases, respectively.

slightly bimodal (see Table II), i.e., this system is more moleculelike than atomlike, despite the topography of its NAPES. Moreover, the MD for Ps^- is more spread out than the ones of H^- and Mu^- , since Ps^- is more weakly bound, and the MD for He is much more compact than the ones for H^- and Mu^- , as the nucleus of the former is doubly charged whereas the nuclei of the latter are singly charged. These results are in general qualitative agreement with the behavior of the one-electron densities reported in Ref. [20]. We must point out that the symmetry breaking in the classical structure implied by the topography of the NAPES and in the shape of the MD is topological [19], in contrast with the symmetry breaking associated with a quantum phase transition across a critical point in the eigenspectrum of the system [49].

Because of the marginalization over r_{12} , the NAPES and MD do not provide explicit information about the correlation between the two identical particles. This kind of information can be retrieved from the CD (16). However, the latter provides radial information, while it is more revealing to examine the angular behavior. Therefore, we transform $D_c(r_{12}|r_{13}, r_{23})$ into $D_c(\theta_{12}|r_{13}, r_{23})$,

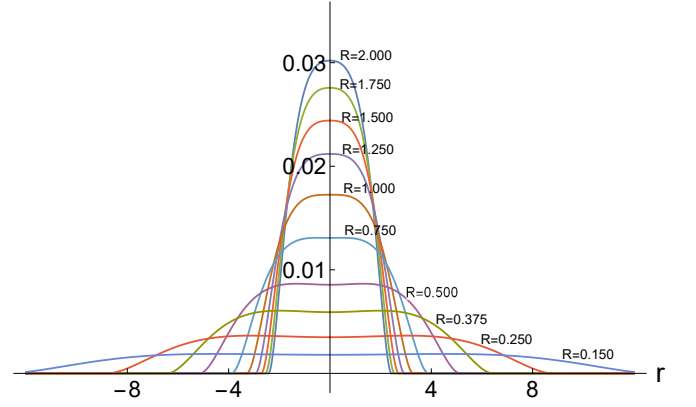


FIG. 4. (Color online) Cuts of the MD's through the line perpendicular to the diagonal ($r_{13} = r_{23}$) and passing through the maximum or maxima, for the model systems (see Table IV). r is the distance from the diagonal.

where θ_{12} is the angle between the lines joining each of the identical particles with the single particle, by means of the relation $r_{12} = (r_{13}^2 + r_{23}^2 - 2r_{13}r_{23}\cos\theta_{12})^{1/2}$. Figure 3 shows the CD's for the realistic systems, evaluated at the maximum or one of the maxima ($r_{13,m}, r_{23,m}$ in Table II) of the corresponding MD for the atomic or molecular cases, respectively. For the atomic systems, H^- and Mu^- , the CD's are almost identical and increase monotonically from the collinear nucleus-electron configuration ($\theta_{12} = 0$) to the collinear electron-nucleus configuration ($\theta_{12} = \pi$) configuration. The minimum at $\theta_{12} = 0$ reveals the so-called Coulomb hole. The probability of finding the electrons at zero separation is identically zero because the MD maximum is on the $r_{13} = r_{23}$ diagonal and, hence, the Jacobian present in Eq. (16) $r_{12} = 0$ when $\theta_{12} = 0$. For the molecular systems, Mu_2^+ and H_2^+ , the CD's have a maximum at $\simeq 90^\circ$ and $\simeq 110^\circ$, respectively, i.e., at this point in the $\{r_{13}, r_{23}\}$ subspace the most probable configuration is bent. The probability of finding the system in the collinear nucleus-nucleus-electron configuration ($\theta_{12} = 0$) now cannot be identically zero because the MD maxima are off the $r_{13} = r_{23}$ diagonal, although for H_2^+ it is practically zero. For Ps^- , the CD is monotonic, albeit much flatter than the ones of H^- and Mu^- , indicating that this system is more delocalized, in accordance with the larger extension of its MD (see Fig. 1). These results are in general qualitative agreement with the angular densities reported in Ref. [20], except that the one of Ps^- appears slightly nonmonotonic, but care must be taken with a direct comparison since those quantities and our CD's are defined differently. In particular, the CD's shown in Fig. 3 are evaluated at specific points of the $\{r_{13}, r_{23}\}$ subspace; their behaviors at other points are different, although not drastically [29].

In Fig. 1 the change in behavior from atomlike to moleculelike is too sudden, due to the abrupt change of the mass ratio (see Table I). In order to visualize the

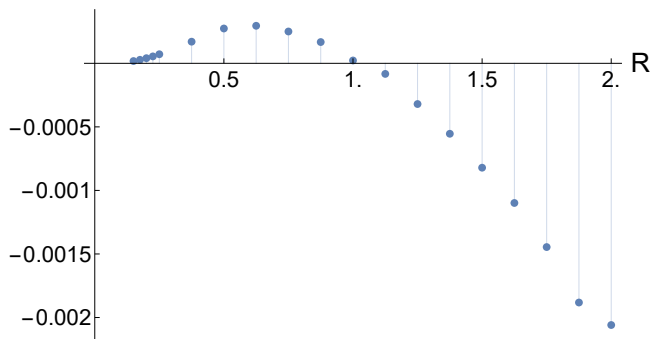


FIG. 5. Second derivatives at the middle points of the cuts of Fig. 4.

transition in a smoother fashion Fig. 4 displays cuts of the MD's through the line perpendicular to the diagonal $r_{13} = r_{23}$ and passing through the single maximum ($R > 1$) or both maxima ($R < 1$), for the series of model systems (see Table IV). It is seen that as $R = m_s$ decreases such cut becomes more spread out, and that at around $R = 1$ it smoothly changes shape from unimodal to bimodal. To characterize more quantitatively this transition, we evaluated the second derivative (SD) at the middle point of each cut, since when the curvature at this point is negative or positive the distribution is unimodal or bimodal, respectively. The results are presented in Table IV and plotted in Fig. 5, where the continuous nature of the transition from atomlike ($R > 1$, $SD < 0$) to moleculelike ($R < 1$, $SD > 0$) can be clearly appreciated. The sign change occurs at $R \simeq 1$ (e.g. Ps^-), which can be taken to mark the boundary between the two types of behavior. Below $R \approx 0.6$ the magnitude of SD decreases towards zero, because the cuts become very spread out.

In Fig. 6 we show the NAPES's and the full MD's for selected model systems. According to Fig. 5, $R = 2$ is the most atomlike system considered and $R = 0.65$, 0.15, 0.05 are moleculelike, with $R = 0.65$ possessing the highest SD value. It is appreciated how the topography of the NAPES gradually deforms, the basins initially being close together and perpendicular, and at the end being more separated and considerably stretched into the diagonal directions (when comparing with Fig. 1 beware of the different scales). Correspondingly, the MD gradually becomes more extended, with its shape at the same time changing from unimodal to bimodal, with the humps more clearly differentiated and located on top of the wells in the NAPES.

V. CONCLUSIONS AND OUTLOOK

After very briefly reviewing the status of the 'molecular structure conundrum' [1, 2, 8–11, 13–18, 24, 25, 32] and stating our own view about the concept of shape for an isolated quantal system, we presented an alternative characterization of the continuous emergence of molecu-

lar shape, as a response to the variation of the particle masses, in prototypical three-particle Coulomb systems.

Our analysis was based mainly on the behaviors of the 2-dimensional nonadiabatic potential energy surface and marginal distribution for the distances between each of the identical particles and the third particle, constructed rigorously by means of a marginal-conditional exact factorization of a variationally optimized internal wavefunction. The analysis was further aided by an examination of the evolution of the variational parameters and the conditional distribution for the angle defined by the two identical particles and the third particle. The classical interpretation of the topography of such surface implies two broken-symmetry indistinguishable equilibrium structures, where the two identical particles move around the single particle along separate orbits. Such topological symmetry breaking is frustrated in the shape of the atomlike systems but preserved in the shape of the moleculelike ones, as revealed by the continuous transition from unimodal to bimodal of the quantum marginal distribution. The conditional distribution, evaluated at selected points of the $\{r_{13}, r_{23}\}$ subspace, was observed to turn from monotonic to nonmonotonic with a single maximum across the transition. The unimodal-bimodal transition has already been observed in cuts of the one-particle extracule densities employed in Refs. [19, 20, 28]. Our characterization has two advantages: First, it is univocal, as it does not rely on the definition of a reference point, in contrast with the one-particle extracule densities, where the bimodality is lost for certain choices of reference points [36, 37]. Second, it permits a unified treatment of atoms, molecules, and any other collection of quantum particles in terms of the potential energy surface concept, which has proven so powerful an interpretive tool in quantum chemistry.

For a three-particle system, alternative marginal-conditional factorizations will generate a different 2-dimensional nonadiabatic potential energy surface or a nonadiabatic potential energy *curve*, which, together with their corresponding marginal and conditional distributions, can be employed to discuss related issues of particle correlation and the nature of the BO approximation.

It has been discovered that certain doubly-excited states of two-electron atoms can be empirically modeled in terms of collective rotational- and bending-like motions of the electrons, analogous to the rovibrational motions of a linear ABA molecule [50] (Ref. [44] reviews this development). In addition, it has been predicted that other doubly-excited states of two-electron atoms adopt classical-like configurations with both electrons on the same side of the nucleus (so-called 'frozen planet' states) [51]. Moreover, it is known that molecules in highly-excited vibrational states can become fluxional. (For a unified review of these three aspects see Ref. [52]). It is very desirable to develop a unified view of these types of system [52]. We feel that our methodology is capable of achieving this goal.

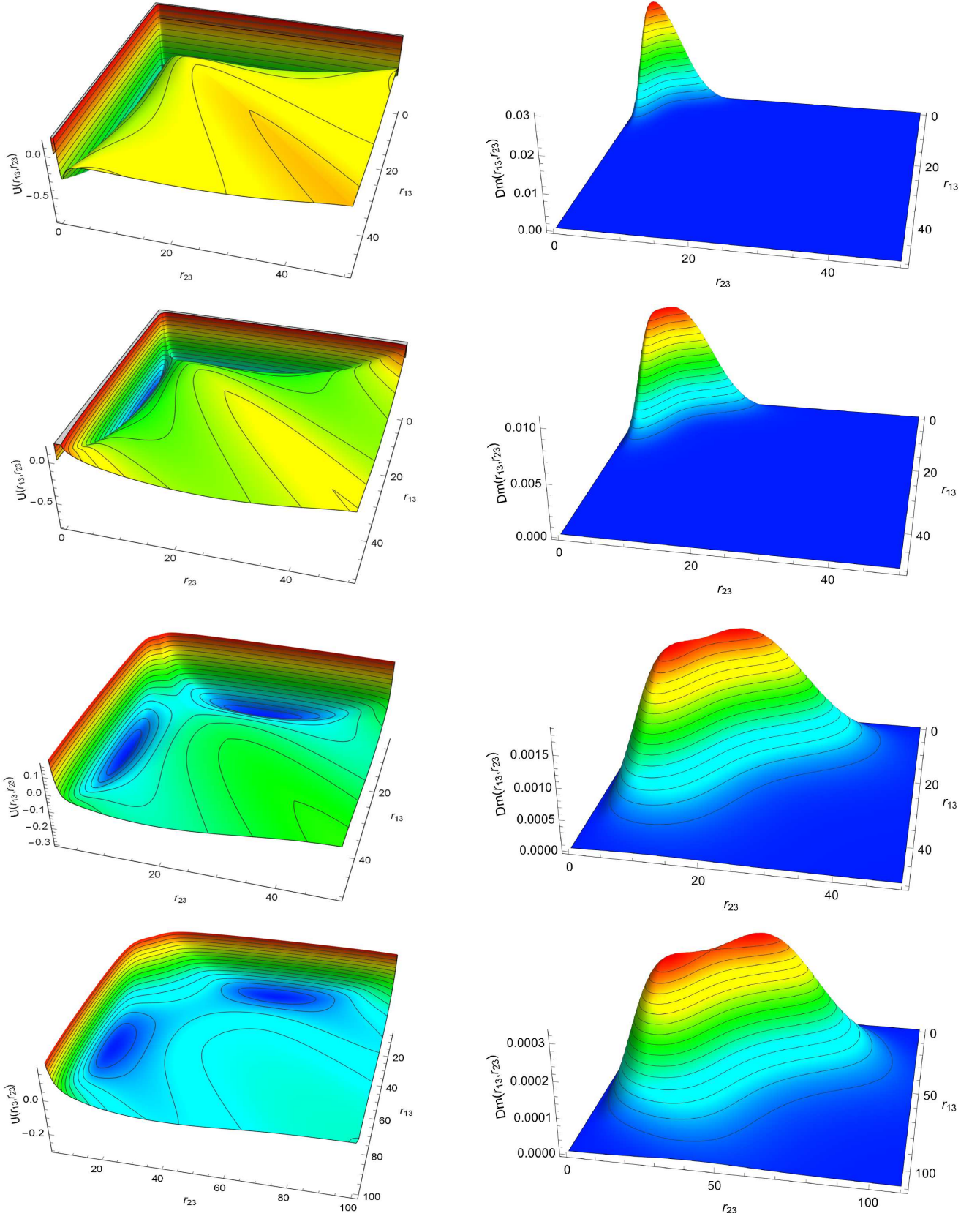


FIG. 6. (Color online) NAPES's (left column) and corresponding MD's (right column) for selected model systems. From top to bottom: $R=2.00, 0.65, 0.15, 0.05$.

ACKNOWLEDGMENTS

Laura D. Salas acknowledges financial support from Colciencias through a doctoral fellowship.

-
- [1] R. G. Woolley, Quantum theory and molecular structure, *Adv. Phys.* **25**, 27 (1976).
- [2] R. G. Woolley, Quantum theory and the molecular hypothesis, in *Molecules in Physics, Chemistry, and Biology*, Vol. 1, edited by J. Maruani (Kluwer, Dordrecht, 1988) pp. 45–89.
- [3] *IUPAC Gold Book Compendium of Chemical Terminology*. <https://goldbook.iupac.org/>. Last accessed on August 6, 2021.
- [4] P. R. Bunker and P. Jensen, *Molecular Symmetry and Spectroscopy*, 2nd ed. (NRC Research Press, Ottawa, 1998).
- [5] P. Coppens, *X-Ray Charge Densities and Chemical Bonding* (Oxford University Press, Oxford, 1997).
- [6] T. McKee and J. R. McKee, *Biochemistry. The Molecular Basis of Life*, 7th ed. (Oxford University Press, Oxford, 2019).
- [7] P. Papon, J. Leblond, and P. H. E. Meijer, *The Physics of Phase Transitions. Concepts and Applications*, 2nd ed. (Springer, Berlin, 2006).
- [8] R. G. Woolley, Must a molecule have a shape?, *J. Am. Chem. Soc.* **100**, 1073 (1978).
- [9] R. G. Woolley, Must a molecule have shape?, *New Scientist* **120**, 53 (1988).
- [10] P. Claverie and S. Diner, The concept of molecular structure in quantum theory: Interpretation problems, *Isr. J. Chem.* **19**, 54 (1980).
- [11] R. G. Woolley, Molecular shapes and molecular structures, *Chem. Phys. Lett.* **125**, 200 (1986).
- [12] B. Sutcliffe and R. G. Woolley, The potential energy surface in molecular quantum mechanics, in *Advances in Quantum Methods and Applications in Chemistry*, edited by M. Hotokka, E. Brändas, J. Maruani, and G. Delgado-Barrio (Springer International Publishing, Switzerland, 2013) pp. 3–40.
- [13] H. Primas, *Chemistry, Quantum Mechanics and Reductionism*, 2nd ed. (Springer-Verlag, Berlin, 1983).
- [14] H. Primas, Emergence in exact natural sciences, *Acta Polytech. Scand.* **Ma 91**, 83 (1998).
- [15] J. C. Martínez-González, S. Fortin, and O. Lombardi, Why molecular structure cannot be strictly reduced to quantum mechanics, *Found. Chem.* **21**, 31 (2019).
- [16] S. J. Weininger, The molecular structure conundrum: Can classical chemistry be reduced to quantum chemistry?, *J. Chem. Ed.* **11**, 939 (1984).
- [17] R. G. Woolley, The molecular structure conundrum, *J. Chem. Ed.* **12**, 1082 (1985).
- [18] M. García-Sucre and M. Bunge, Geometry of a quantal system, *Int. J. Quant. Chem.* **19**, 83 (1981).
- [19] E. Mátyus, J. Hutter, U. Müller-Herold, and M. Reiher, On the emergence of molecular structure, *Phys. Rev. A* **83**, 052512 (2011).
- [20] E. Mátyus, J. Hutter, U. Müller-Herold, and M. Reiher, Extracting elements of molecular structure from the all-particle wave function, *J. Chem. Phys.* **135**, 204302 (2011).
- [21] P. Cassam-Chenaï and E. Mátyus, Electrons as an environment for nuclei within molecules: a quantitative assessment of their contribution to a classical-like molecular structure, arXiv:2011.10312 [physics.chem-ph].
- [22] E. Mátyus and P. Cassam-Chenaï, Orientational decoherence within molecules and emergence of the molecular shape, *J. Chem. Phys.* **154**, 024114 (2021).
- [23] C. Zhong and F. Robicheaux, Decoherence of rotational degrees of freedom, *Phys. Rev. A* **94**, 052109 (2016).
- [24] S. Fortin, O. Lombardi, and J. C. Martínez-González, Isomerism and decoherence, *Found. Chem.* **18**, 225 (2016).
- [25] A. Franklin and V. Seifert, The problem of molecular structure just is the measurement problem, *Br. J. Philos. Sci.*, forthcoming. Downloaded from kcl.ac.uk.
- [26] M. Schlosshauer, *Decoherence and the Quantum-to-Classical Transition* (Springer, Berlin, 2007).
- [27] J. C. Arce, Unification of the conditional probability and semiclassical interpretations for the problem of time in quantum theory, *Phys. Rev. A* **85**, 042108 (2012), version with typographical errors corrected: arXiv:1202.4638v3 [quant-ph].
- [28] A. L. Baskerville, A. W. King, and H. Cox, Quantum effects of nuclear motion in three-particle diatomic ions, *Phys. Rev. A* **94**, 042512 (2016).
- [29] L. D. Salas and J. C. Arce, Potential energy surfaces in atomic structure: The role of Coulomb correlation in the ground state of helium, *Phys. Rev. A* **95**, 022502 (2017).
- [30] E. Mátyus, Pre-Born–Oppenheimer molecular structure theory, *Mol. Phys.* **117**, 590 (2018).
- [31] P. Cassam-Chenaï, Conditional probability amplitudes in wave mechanics, *Int. J. Quant. Chem.* **9**, 237 (1975).
- [32] E. B. Wilson, On the definition of molecular structure in quantum mechanics, *Int. J. Quant. Chem. Symp.* **13**, 5 (1979).
- [33] P. Cassam-Chenaï, On non-adiabatic potential energy surfaces, *Chem. Phys. Lett.* **420**, 354 (2006).
- [34] N. I. Gidopoulos and E. K. U. Gross, Electronic non-adiabatic states: towards a density functional theory beyond the Born–Oppenheimer approximation., *Phil. Trans. R. Soc. A* **372**, 20130059 (2014).
- [35] A. Abedi, N. T. Maitra, and E. K. U. Gross, Correlated electron-nuclear dynamics: Exact factorization of the molecular wavefunction, *J. Chem. Phys.* **137**, 22A530 (2012).
- [36] C. G. Rodríguez, A. S. Urbina, F. J. Torres, D. Cazar, and E. V. Ludeña, Non-Born–Oppenheimer nuclear and electronic densities for a three-particle Hooke–Coulomb model, *Comput. Theor. Chem.* **1018**, 26 (2013).
- [37] M. Becerra, V. Posligua, and E. V. Ludeña, Non-Born–Oppenheimer nuclear and electronic densities for a Hooke–Coulomb model for a four-particle system, *Int. J. Quant. Chem.* **113**, 1584–1590 (2013).
- [38] A. W. King, L. C. Rhodes, and H. Cox, Inner and outer

- radial density functions in correlated two-electron systems, *Phys. Rev. A* **93**, 022509 (2016).
- [39] A. A. Frost, The use of interparticle coordinates in electronic energy calculations for atoms and molecules, *Theor. Chim. Acta* **1**, 36 (1962).
- [40] E. A. Hylleraas, Neue Berechnung der Energie des Heliums im Grundzustande, sowie des tiefsten Terms von Ortho-Helium., *Z. Phys.* **54**, 347 (1929), an English translation of this paper can be found in *Quantum Chemistry. Classic Scientific Papers*, translated and edited by H. Hettema (World Scientific, Singapore, 2000).
- [41] E. A. Hylleraas, The Schrödinger two-electron atomic problem, *Adv. Quantum Chem.* **1**, 1 (1964).
- [42] A. M. Frolov, Bound-state calculations of coulomb three-body systems, *Phys. Rev. A* **59**, 4270 (1999).
- [43] I. N. Levine, *Quantum Chemistry*, 7th ed. (Pearson, Upper Saddle River, 2014).
- [44] R. S. Berry, Probing the collective and independent-particle character of atomic electrons, in *Structure and Dynamics of Atoms and Molecules: Conceptual Trends*, edited by J. L. Calais and E. S. Kryachko (Springer Science+Business Media, Dordrecht, 1995) pp. 155–181.
- [45] T. Jecko, B. T. Sutcliffe, and R. G. Woolley, On factorization of molecular wavefunctions, *J. Phys. A: Math. Theor.* **48**, 445201 (2015).
- [46] G. H. Gossel, L. Lacombe, and N. P. Maitra, On the numerical solution of the exact factorization equations, *J. Chem. Phys.* **150**, 154112 (2019).
- [47] A. Flores-Riveros and J. F. Rivas-Silva, Variational description of the 3-body Coulomb problem through a correlated Eckart-Gaussian wavefunction, *Braz. J. Phys.* **29**, 529 (1999).
- [48] Wolfram Research, Inc., *Mathematica*, Version 12.0 (2020).
- [49] Q. Shi and S. Kais, Quantum criticality at the large-dimensional limit: Three-body Coulomb systems, *Int. J. Quant. Chem.* **85**, 307 (2001).
- [50] M. E. Kellman and D. R. Herrick, Ro-vibrational collective interpretation of supermultiplet classifications of intrashell levels of two-electron atoms, *Phys. Rev. A* **22**, 1536 (1980).
- [51] K. Richter, J. S. Briggs, D. Wintgen, and E. A. Solov'ev, Novel dynamical symmetries of asymmetrically doubly excited two-electron atoms, *J. Phys. B: At. Mol. Opt. Phys.* **25**, 3929 (1992).
- [52] M. E. Kellman, Nonrigid systems in chemistry: A unified view, *Int. J. Quant. Chem.* **65**, 399 (1997).